

NASA Technical Paper 1729

NASA  
TP  
1729  
c. 1

LOAN COPY  
AFWL TECH  
KIRTLAND

0134872



**WIND - Computer Program for  
Calculation of Three-Dimensional  
Potential Compressible Flow  
About Wind Turbine Rotor Blades**

Djordje S. Dulikravich

OCTOBER 1980

**NASA**



NASA Technical Paper 1729

**WIND - Computer Program for  
Calculation of Three-Dimensional  
Potential Compressible Flow  
About Wind Turbine Rotor Blades**

Djordje S. Dulikravich  
*Lewis Research Center  
Cleveland, Ohio*

**NASA**

National Aeronautics  
and Space Administration

**Scientific and Technical  
Information Branch**

1980

## Summary

A computer program (WIND) has been developed that numerically solves an exact, full-potential equation (FPE) for three-dimensional, steady, inviscid flow through an isolated wind turbine rotor. The program automatically generates a three-dimensional, boundary-conforming grid and iteratively solves the FPE while fully accounting for both the rotating cascade and Coriolis effects. The numerical techniques incorporated involve rotated, type-dependent finite differencing, a finite volume method, artificial viscosity in conservative form, and a successive line overrelaxation combined with the sequential grid refinement procedure to accelerate the iterative convergence rate. Consequently WIND is capable of accurately analyzing incompressible and compressible flows, including those that are locally transonic and terminated by weak shocks. WIND can also be used to analyze the flow around isolated aircraft propellers and helicopter rotors in hover as long as the total relative Mach number of the oncoming flow is subsonic.

## Introduction

An exact, full-potential equation (FPE) that governs three-dimensional steady, inviscid, potential flow through the wind turbine rotor can be expressed in the following vector form (refs. 1 and 2):

$$a^2 \Delta^2 \varphi - (\Delta \varphi \cdot \Delta) \frac{1}{2} (\Delta \varphi \cdot \Delta \varphi) + 2(\Delta \varphi \cdot \Delta)((\Omega \times \mathbf{r}) \cdot \Delta \varphi) - ((\Omega \times \mathbf{r}) \cdot \Delta)((\Omega \times \mathbf{r}) \cdot \Delta \varphi) = 0 \quad (1)$$

where  $\mathbf{V} = \Delta \varphi$  is the absolute velocity vector defined as

$$\mathbf{V} = \mathbf{V}_r + \Omega \times \mathbf{r} \quad (2)$$

Here  $\mathbf{V}_r$  is the relative velocity vector of the fluid with respect to the rotating blade,  $\Omega$  is the angular rotor speed, and  $\mathbf{r}$  is the position vector in the rotor plane.

Equation (1) is a second-order, quasi-linear, partial differential equation of mixed elliptic-hyperbolic type. For the particular set of boundary conditions the solution of FPE can be composed of locally hyperbolic regions (supersonic relative flow) that neighbor regions where FPE is locally of an elliptic

type (i.e., where the local relative flow is subsonic). The boundary surfaces separating these regions can be of a continuous parabolic type (sonic surfaces) or of a mathematically discontinuous type (isentropic shocks). This means that the FPE can govern flow regimes varying from incompressible (when the FPE reduces to a simple Laplace's equation) through the transonic, accepting mathematical discontinuities in the "weak solution" form. These discontinuities are then interpreted as weak isentropic shocks (refs. 3 and 2).

The FPE cannot be solved analytically, and therefore a numerical method will be used. This method, called the finite-volume method (refs. 4 and 5), represents a combination of finite difference and finite element techniques. Because of the exceedingly large number of mathematical operations that will be performed and the large amount of computer storage required, an iterative, successive line overrelaxation (SLOR) technique is used. The details of the numerical scheme have been presented in other references (refs. 6, 7, and 2) and will not be repeated in this users manual. To make the computer program suitable for computers with a limited central memory, the program was written in such a way that a number of disks or tapes will accommodate the excessive storage requirements.

## Applicability of Computer Program WIND

The computer program WIND is capable of numerically analyzing the flow field about a given blade shape of the wind turbine rotor (horizontal-axis type).

The rotor hub is defined as a doubly infinite circular cylinder having the  $x$  coordinate as its axis. An arbitrary number of blades can be attached to the hub. The blades can have arbitrary spanwise distribution of taper and of the twist, sweep, and dihedral angles. An arbitrary number of different airfoil section shapes can be used along the span, although the spanwise variation of all the geometric parameters must be reasonably smooth.

The results of the numerical analysis are given in the form of a computer printout. At a number of spanwise stations along the blade the output gives the chordwise distribution of the coefficient of pressure,

the Mach number, the density, and the relative velocity vector components. In addition, the results specify local values of the lift coefficient and tangential and axial aerodynamic force components. These are also given in an integrated form expressing the total torque on the shaft and the total axial force on the shaft.

As stated in reference 8, WIND numerically solves an exact, full-potential equation for a three-dimensional, steady, homentropic flow of an inviscid, compressible, homocompositional, non-radiating, and nonconducting fluid. The practical implications of this mathematical model are the following:

(1) The wind is blowing at a steady speed. Gusts lasting for a period of time long enough to change the loading of the blade significantly should be analyzed as separate test cases at different wind speeds, each speed treated as a different constant.

(2) The axis of the rotor is always aligned with the wind.

(3) The atmospheric turbulence is of negligible intensity.

(4) The tower and all other obstacles are placed downwind from the rotor.

(5) The entire rotor is placed above the ground shear layer; that is, the wind speed is uniform.

(6) Vertical and horizontal variations of atmospheric density and temperature are negligible.

(7) The rotor rotates at constant angular speed.

(8) There is no separation of the airstream from the blades or the rotor hub.

(9) The rotor hub has the shape of an infinitely long, circular cylinder.

(10) Atmospheric impurities (rain, snow, ice, sand, dust, and industrial air pollutants) are uniformly distributed throughout the air mass.

It is important to explicitly warn the users of the WIND code that this program cannot account for possible flow separations and subsequent heavy losses due to poor aerodynamic design of rotor blades.

In its present form WIND is capable of calculating flow fields that could become locally supersonic and terminate with weak shocks. Although this situation is not desirable, it can easily occur in the case of a strong gust or a malfunction of the blade twisting (pitching) mechanism. The consequences include an unacceptably high level of noise and possibly serious damage to the blade and tower structure as the result of an aerodynamic load that was not accounted for during the blade design process.

With increasing rotor diameter and angular speed the outer portions of the blades will operate in a flow regime where the compressibility effects cannot be neglected. The compressibility effects, combined

with blade shapes incorporating advanced shockless airfoil shapes, are capable of significantly increasing the aerodynamic efficiency of the rotor without increasing the noise level. The theories for this approach have already been developed (refs. 9 and 10) and successfully tested numerically (ref. 11).

Besides being capable of calculating flows ranging from the incompressible through the transonic regime, WIND fully accounts for the effect of the Coriolis force and the mutual blade interference (cascade) effect. Compressibility and Coriolis effects will be important in the outer portion of the blade; the three-dimensional rotating cascade effects become important in the blade root region.

## Global Structure of Program

A computer program called WIND numerically solves the FPE. The program is written in FORTRAN IV and consists of about 2200 computer cards. Wind automatically generates the computational grids and performs the iterative solution of the FPE. Thus user intervention is unnecessary once the program has begun execution.

While developing and testing the program it was observed that the computational grid-generating portion of the code uses about 50 percent of the total high-speed memory required by WIND but consumes less than 2 percent of the total central processing unit time required by WIND. Therefore, to save computer storage and at the same time provide the designer with an opportunity to separately analyze the geometry, WIND was divided into two separate programs (fig. 1).

The first portion of this code is called WIND-01. It reads its own input data, which contain all major geometric parameters. WIND-01 then generates the three-dimensional, body-fitted grid and stores it on disks or tapes.

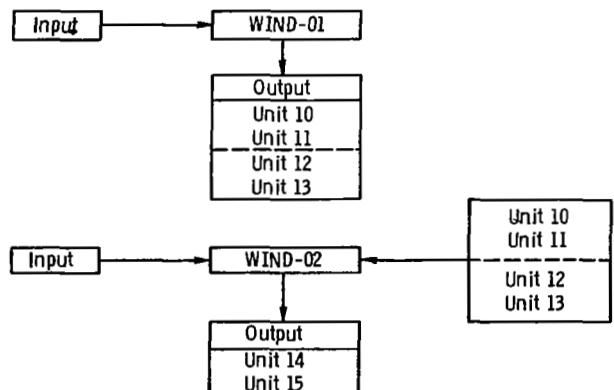


Figure 1. - Global flow chart.

The second portion of the program is called WIND-02. It reads the  $(x,y,z)$  coordinates that were previously generated by WIND-01 and thus reactivates units 10, 11, 12, and 13. WIND-02 also reads its own input, which defines the basic flow parameters, and then performs an iterative solution of the FPE. The final results of WIND are thus the results of WIND-02. These results, representing values of the potential function, will remain stored on units 14 and 15.

## Computer Program WIND-01

The grid generation performed by WIND-01 is based on an analytic function (refs. 12 and 2) that conformally maps a cascade of straight slits onto a cascade of unit circles with a slit in the middle (fig. 2). These circles are "unwrapped" by using elliptic polar coordinates. After additional coordinate stretching and shearing this deformed rhomboid is converted into a parallelepiped-shaped computational domain suitable for finite differencing. Several important geometric parameters and  $(x,y,z)$  coordinates of the coarse (first) grid are stored permanently on units 10 and 11, coordinates of the refined (second) grid are stored on unit 12, and coordinates of the fine (third) grid are stored on unit 13 so that each of them can be separately plotted and analyzed.

The computer program WIND-01 consists of seven routines and a separate input data operation (fig. 3). The input data are discussed in detail in the following section. The subroutine MAIN is the principal part

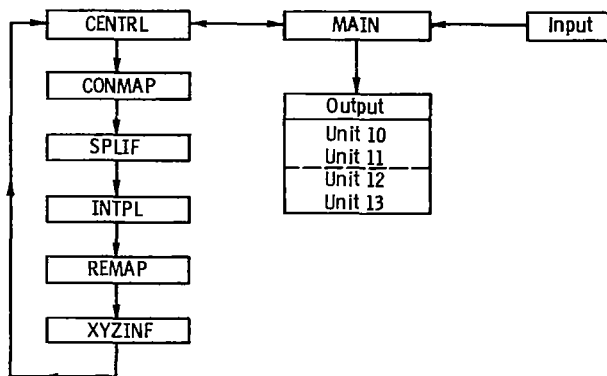


Figure 3. - Flow chart of WIND-01 computer program.

of WIND-01 in the sense that most of the other routines are called from that routine. MAIN reads the input data and rotates the airfoil to its actual stagger angle. MAIN also writes  $(x,y,z)$  coordinates of the first (coarse) grid on unit 11 and the values of the parameters XCELL, YCELL, ZCELL, RHUB RTIP, RINF, TIPCEL, and BLADE (explained in the following section) on unit 10. On the same unit 10, MAIN also writes the values of the normalized radii of the cylindrical computational surfaces (ref. 8) intersecting the blade. If the original coarse grid has to be refined in all three directions, the refined grid coordinates will automatically be written onto unit 12. The coordinates of the fine (third) grid will be written by MAIN on unit 13.

Subroutine CENTRL calculates the length of the central slit in the circle plane and calls routines SPLIF, INTPL, CONMAP, and REMAP in order to perform the conformal mapping and remapping.

Subroutine CONMAP iteratively performs the point-by-point conformal mapping from the  $(x,\theta)$  plane onto the circle plane. Furthermore CONMAP "unwraps" the circle and calculates the elliptic polar coordinates (fig. 2).

Subroutine SPLIF fits a cubic spline through the lower boundary of the computational domain that corresponds to the surface of the airfoil.

Subroutine INTPL interpolates the values of the elliptic polar coordinates at points that are equidistantly spaced with respect to the image of the upstream infinity. This is a necessary step in obtaining a grid that is periodic in the  $\theta$ -direction.

Subroutine REMAP analytically determines coordinates of the mesh points in the physical plane; that is, REMAP performs a backtransformation process from the computational plane to the  $(x,\theta)$  plane.

The mesh points defining the axial infinities should be positioned along the line  $x=\text{constant}$  (fig. 4). Because of the way the potential jump  $\Gamma$  will be enforced across the cut, the points at  $x = +\infty$  should be

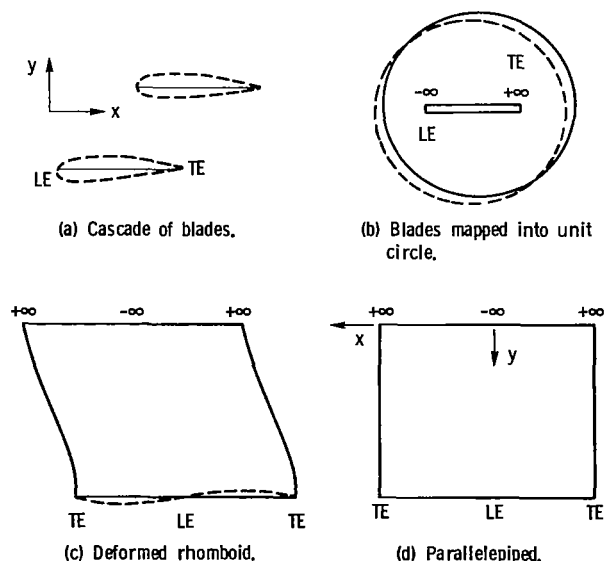


Figure 2. - Transformation from  $(x,\theta)$  plane into computational plane, where TE denotes trailing edge and LE denotes leading edge.

equidistantly positioned in the  $\theta$  direction with respect to that cut.

Subroutine XYZINF determines the coordinates of the axial infinity points explicitly, because they cannot be obtained from the conformal mapping. XYZINF also determines the coordinates of points in the imaginary rows and columns outside the actual computational domain.

#### Input to WIND-01

All the input data for WIND-01 are combined in one data set (see appendix A). Following is a card-by-card description of that data set (see appendix B for the input format).

The first card contains an arbitrary text composed of up to 80 alphanumeric characters. Its purpose is to give a description or a name to the entire input defining the blade geometry. This same text will then appear at the beginning of the output of WIND-01.

The second card contains the following five parameters:

- XCELL** number of computational mesh cells around surface of each blade cross section (fig. 4) when calculating on coarse (first) grid. XCELL must be an even number. The maximum suggested value is XCELL = 24.
- YCELL** number of elliptic layers of mesh cells enveloping each local blade cross section (fig. 4) when calculating on a coarse grid. The suggested minimum value is YCELL = 5.
- ZCELL** number of mesh cells in spanwise direction (between hub and radial in-

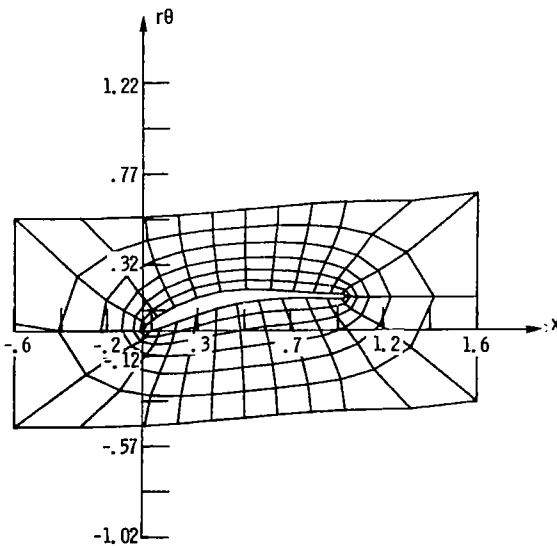


Figure 4. - Computational mesh on  $(x, r\theta)$  cylindrical surface.

finity cutoff boundary) when calculating on coarse grid. The minimum value for ZCELL that will still provide for a stable numerical scheme can be determined from the following expression:

$$ZCELL = 0.9 \left( \frac{r_t - r_h}{c_t + c_h} \right) + 2.$$

where  $r_t$  is the rotor radius,  $r_h$  is the radius of the rotor hub,  $c_h$  and  $c_t$  are the blade chord lengths at the hub and the tip, respectively.

**TIPCEL** number of mesh cells in spanwise direction (between hub and the tip of blade) when calculating on coarse grid. The maximum value for TIPCEL should be

$$TIPCEL = ZCELL - 2.$$

**PMESH** total number of consecutively refined computational grids that should be generated and separately stored. The number of the mesh cells on the first (coarse) three-dimensional grid is defined by specifying XCELL, YCELL, ZCELL, and TIPCEL. Each following grid will be automatically generated with twice as many mesh cells in each of the computational directions  $(X, Y, Z)$  as the previous grid had. The minimum value for PMESH is 1 and the maximum value is 3.

The third input card contains the following five parameters:

- RINF** normalized radius of cylindrical outer boundary on which radial infinity boundary conditions will be applied (ref. 8). Normalization must be performed with respect to the rotor radius  $r_t$  (fig. 8).
- RHUB** normalized radius of rotor hub. Again, the normalizing length is  $r_t$ .
- RTIP** rotor radius  $r_t$ , ft
- BLADE** number of rotor blades
- SETANG** blade setting angle, deg. This is the angle between the pitching position of the blade as defined by the rest of the input data and any other blade pitching position (fig. 5).

The actual detailed shape of the blade without the hub is given on a number of  $(x, y)$  input planes (fig. 6). The innermost input plane must be positioned inside the hub; the outermost input plane should be positioned precisely at or beyond the blade tip.

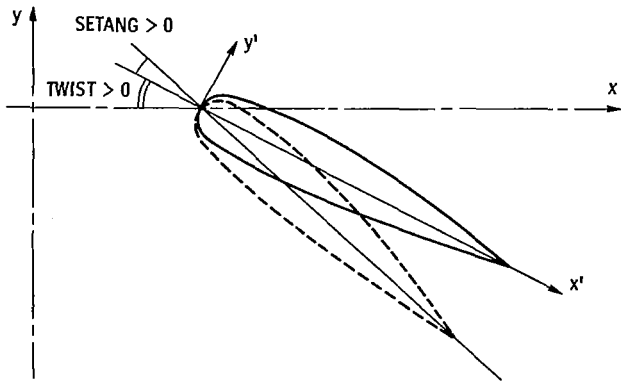


Figure 5. - Local blade section inclination.

The fourth input card contains eight parameters defining the relative position in space of the  $N^{th}$  local blade cross section. These parameters are

- N** number of  $(x,y)$  input plane. The planes are numbered in the spanwise direction, starting with  $N=1$  for the most inward plane (fig. 6). The maximum number of input planes  $N=NP$  is 25.
- RLEAD** radial distance from axis of rotation to leading edge of local airfoil defined on  $N^{th}$  plane. RLEAD is nondimensional; the normalizing length being the rotor radius RTIP.
- CHORD** chord length of blade local cross section defined on  $N^{th}$  input plane. Chord length is defined as a maximum distance connecting the leading and trailing edges of the blade section. CHORD is nondimensionalized with respect to RTIP.
- XLEAD** axial distance (sweep) from origin of  $(x,y,z)$  coordinate system to leading edge of the blade cross section defined on  $N^{th}$  plane. The origin should be placed on the axis of rotation ( $x$  axis) close to the point of intersection of an extrapolated leading edge and that axis (fig. 6). XLEAD is nondimensionalized with respect to the RTIP.
- R01,R02** leading- and trailing-edge radii of blade local cross-section (airfoil) shape defined in  $N^{th}$  plane. R01 and R02 are nondimensionalized with respect to the actual local blade chord length on the  $N^{th}$  plane.
- TLEAD** local dihedral angle between  $z$  axis and leading edge of blade cross section on  $N^{th}$  plane (fig. 6), deg
- TWIST** local twist angle between  $x$  axis and line connecting leading and trailing edges of blade cross section defined on  $N^{th}$  plane (figs. 5 and 6), deg

The fifth input card, together with a number of following input cards, specifies pairs of  $(x',y')$  coordinates of the finite number of input points defining the shape of a local blade cross section on the  $N^{th}$  plane. These cards also specify the number of each point and a control parameter (explained below) assigned to each input point. Thus the input parameters appearing on the fifth card (and several consecutive input cards) are (appendix A):

- I** number of particular point on local airfoil surface at  $N^{th}$  station. The input points are numbered starting from the trailing edge ( $I=1$ ) and proceeding clockwise until the trailing-edge point is reached again ( $I=MAXP$ ). The maximum number of input points at each  $N^{th}$  station is  $MAXP=65$ . By increasing the length of vector arrays in COMMON/BLK1/ and COMMON/BLK2/ of the WIND-01 code, the value of  $MAXP$  can be increased accordingly.
- $x'$**   $x'$  coordinate of  $I^{th}$  input point on blade cross section at  $N^{th}$  spanwise station. The value of  $x'$  is normalized with respect to the local blade chord length. The range of possible  $x'$  values is  $0 < x' < 1$ .
- $y'$**   $y'$  coordinate of  $I^{th}$  input point on blade cross section at  $N^{th}$  spanwise station. The value of  $y'$  is normalized with respect to the local blade chord length.

It is emphasized that the  $(x',y')$  input system differs from the  $(x,y,z)$  coordinate system (fig. 5). The  $(x',y')$  system is attached to the local leading edge of the  $N^{th}$  blade cross section, with the  $x'$  axis passing through the blade leading- and trailing-edge points. The  $(x,y,z)$  system has its origin on the axis of rotation ( $x$  axis) and rotates with the blade.

As already mentioned, the fifth card and each number of the following input cards specify  $x'$  and  $y'$  coordinates of two input points (appendix A). The total number of input points on each  $N^{th}$  plane must be odd (counting the trailing-edge point twice, i.e.,

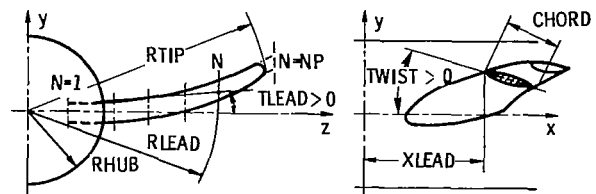


Figure 6. - Local spanwise input parameters.

accounting for it as  $I=1$  and  $I=MAXP$ ) if the local airfoil shape is not symmetrical. If the local input airfoil shape is symmetrical, the total number of input points must be even, and only the points along the lower airfoil surface need be specified. WIND-01 will then automatically determine the symmetrically positioned remaining input points that are on the upper blade surface.

From appendix A it can be seen that after each pair of  $(x',y')$  coordinates specifying an input point on the  $N^{th}$  station, there is a three-digit parameter. Its description follows:

**NEXT** input reading parameter. The value NEXT = 111 at the end of each input card specifying  $(x',y')$  input coordinates means that the following input card has the same format and that the reading of input data of the same type can be continued. The value NEXT = 000 acknowledges the end of the set of input cards specifying  $(x',y')$  coordinates and consequently the end of all the data that are needed at the  $N^{th}$  station. Such a set involves input card 4 and all the following cards, including a card with NEXT = 000. A value of NEXT = 222 at the end of such a set of cards instead of NEXT = 000 means that the airfoil shape at the  $(N+1)^{th}$  station will be the same as it was at the  $N^{th}$  station.

An entire set of  $(x',y')$  input coordinates has to be formed for each of the  $N$  spanwise input stations. Only when the last parameter on the  $N^{th}$  station input set is NEXT = 222 will the set for the  $(N+1)^{th}$  station consist of a single input card having the format of the fourth input card.

The very last card in the input deck for the WIND-01 code is the same as card 4, but with N specified as  $N=0$ . The rest of the parameters on that card are arbitrary (appendix A).

#### Output of WIND-01

The results of the WIND-01 program are partially given in written form on a single page of standard computer output (appendix C). This output lists the name of the programmer, the name of the program, and the institution where it was developed. These statements are followed by a listing of major geometric input parameters defining each  $N^{th}$  spanwise station. This listing is helpful in debugging the input deck. The next portion of printed output gives the following parameters, obtained after the spanwise interpolation has been performed:

<b>K</b>	number of cylindrical computational surface (fig. 8)
<b>RADII</b>	radii of $K^{th}$ cylindrical computational surface divided by rotor radius (RTIP).
<b>TWIST</b>	twist angle of intersection contour (profile) obtained by intersecting blade with $K^{th}$ cylindrical computational surface, deg
<b>CHORD</b>	chord length of the contour at $K^{th}$ station. CHORD is normalized with respect to RTIP.
<b>XL</b>	axial distance between origin of $(x,y,z)$ coordinate system and leading edge of contour on $K^{th}$ cylindrical surface. XL is normalized with respect to RTIP.
<b>TL</b>	tangential distance between $z$ axis and leading edge of contour on $K^{th}$ cylindrical surface, deg

The major portion of the output from WIND-01 will be permanently stored on disks or tapes (fig. 3). For example, the parameters XCELL, YCELL, ZCELL, RHUB, RTIP, RINF, TIPCEL, and BLADE and the normalized radii of the  $K$  computational cylindrical surfaces will be stored on unit 10. The  $(x,y,z)$  coordinates defining every mesh point on the coarse three-dimensional grid will always be stored on unit 11. The  $(x,y,z)$  coordinates of the next (refined) three-dimensional grid will be automatically defined and stored on unit 12 (if PMESH = 2). If PMESH = 3 in the input data, the  $(x,y,z)$  coordinates of the fine (third) grid will be automatically generated and stored on unit 13. A message will appear on the print-out sheet each time a separate storage device has been successfully used.

### Computer Program WIND-02

The second part of the program WIND, called WIND-02, is executed separately after the  $(x,y,z)$  coordinates of the body-conforming grid have been generated by the first part, WIND-01. The purpose of WIND-02 is to actually solve the exact full-potential equation and to calculate important aerodynamic parameters characterizing the flow field. WIND-02 was written in a modular form, separating the main steps in the solution process of the governing equation (fig. 7).

The main program, which reads input data that are written on cards as well as the  $(x,y,z)$  coordinates of the computational grid generated by WIND-01, is called MAIN. The same routine calls other routines and refines the potential field after the iteration process on a particular mesh has converged (when PMESH is greater than 1).



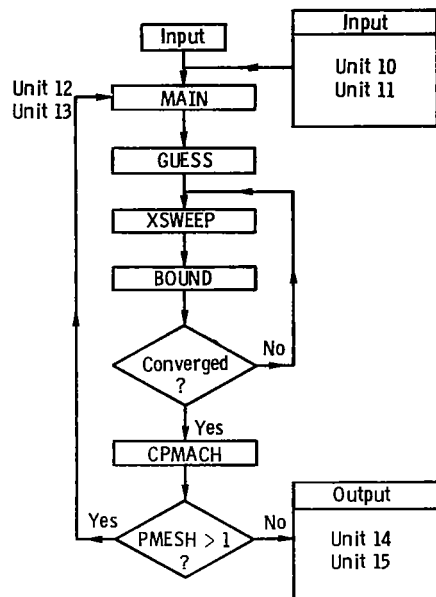


Figure 7. - Flow chart of WIND-02 computer program.

In order to generate an improved initial guess for the potential field calculation on a first (coarse) mesh, subroutine GUESS is called. GUESS iteratively solves an exact two-dimensional full potential equation of the form (ref. 13)

$$(a^2 - \varphi_{,x}^2)\varphi_{,xx} + (a^2 - \varphi_{,y}^2)\varphi_{,yy} - 2\varphi_{,x}\varphi_{,y}\varphi_{,xy} = 0 \quad (3)$$

Here the  $x$  coordinate corresponds to the  $x$  coordinate in the  $(x, y, z)$  space, and the  $\bar{y}$  coordinate represents an arc length; that is

$$\bar{y} = r\theta \quad (4)$$

where  $r$  is the radius of the  $K^{th}$  cylindrical surface and  $\theta$  is the angle between the  $z$  axis and the point in question (fig. 8). The maximum number of  $K$  cylindrical surfaces is 24 in the present version of WIND.

Subroutine XSWEPT iteratively performs the actual flow calculation by using the SLOR technique. XSWEPT uses type-dependent rotated finite differencing and the artificial time concept in order to evaluate coefficients of the tridiagonal correction to the potential matrix. The residues are evaluated by using the finite area technique. The artificial viscosity is added explicitly in conservative form.

Subroutine BOUND applies boundary and periodicity conditions after each complete sweep through the flow field performed by XSWEPT. BOUND is also called after each mesh refinement.

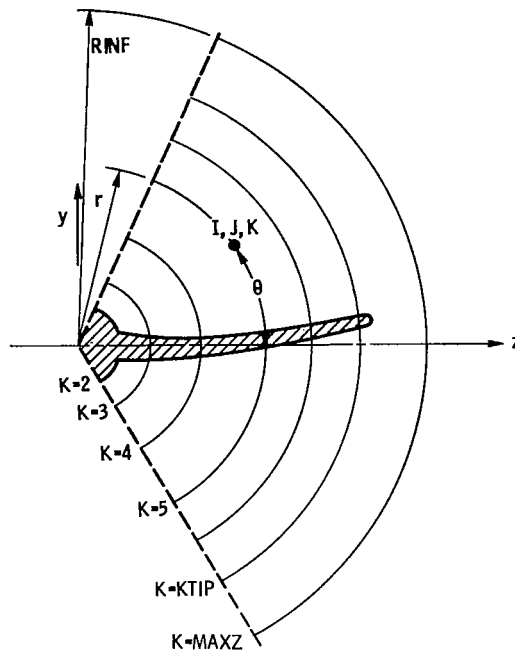


Figure 8. - Cylindrical computational planes.

Subroutine CPMACH calculates the chordwise distribution of the coefficient of pressure, the local relative Mach number, the density, and the relative velocity components at each  $K^{th}$  spanwise station. CPMACH also integrates the coefficient of pressure and gives the force and moment distribution along the blade.

#### Input to WIND-02

The input to WIND-02 is composed of two separate parts. The first part of the input consists of the following four computer cards (appendix D):

The first input card is the so-called title card, meaning that the name of the test case or some other text not longer than 80 alphanumeric characters can be written on that card (see appendix E for formatting).

The second input card specifies the following three input parameters:

UNIF	wind speed, mph
OMEGA	angular speed of rotor, rpm
TEMP	temperature of air, °F

The third input card specifies CONVER, RLX, and PMESH, where

CONVER circulation rate of convergence criteria in case of lifting flows

$$CONVER = \frac{\Gamma^{n+1} - \Gamma^n}{\Gamma^n}$$

where  $\Gamma^n$  is the value of the circulation at the particular spanwise sta-

RLX      tion. The suggested input value for CONVER is  $CONVER = 1.0D - 05$ . iterative overrelaxation factor in regions of locally subsonic relative flow. If the calculation is going to be performed on more than one grid, the value of RLX will automatically be increased by 5 percent on each following (refined) grid. Suggested value is  $RLX = 1.65$ .

PMESH    total number of computational grids used. Minimum value is  $PMESH = 1$ . With the common region presently existing in WIND-01 and WIND-02, the maximum value for PMESH is  $PMESH = 3$ . This means that the calculation can be performed on a coarse grid consisting of  $(24 \times 6 \times ZCELL)$  mesh cells and then automatically continued on two more consecutively three-dimensionally refined grids. Calculation on a single coarse grid ( $PMESH = 1$ ) usually gives quite satisfactory results.

The fourth input card contains values for ITER1, ITER2, and PRESS, where

ITER1    maximum number of iterations to be performed on first (coarse) grid. The suggested value is  $ITER1 = 50$ .

ITER2    maximum number of iterations to be performed on second grid (if  $PMESH > 1$ ). The suggested value is  $ITER2 = 30$ . If three grids are to be used ( $PMESH = 3$ ), the maximum value of iterations on the third grid will be automatically determined as  $ITER3 = ITER2/2$ .

PRESS    atmospheric pressure, lb/in<sup>2</sup>, usually about  $PRESS = 14.7$

The second portion of the input to the WIND-02 program consists of the  $(x,y,z)$  coordinates previously generated by WIND-01 and stored on units 10, 11, and possibly 12 and 13. These units of permanent storage will be used during the entire execution of WIND-02.

#### Output from WIND-02

The results of the iterative solution of an exact full-potential equation as obtained by WIND-02 are given in printed form. The  $(x,y,z)$  coordinates of the computational grid (or grids, if  $PMESH > 1$ ) will remain saved on units 10 and 11 (and possibly 12 and 13). Thus, if WIND-02 is run again for the same blade geometry, but with different input parameters (UNIF, OMEGA, TEMP, and PRESS), the time and

money for executing WIND-01 can be saved. Besides saving  $(x,y,z)$  coordinates of the computational grid, the values of the reduced potential  $G(x,y,z)$  defined as

$$\varphi(x,r,\theta) = \frac{1}{(q^2)_{-\infty}} (UNIF*x + OMEGA*r) + G(x,y,z) \quad (5)$$

will remain saved on units 14 and 15, which were used during the execution of WIND-02.

These values of  $G(x,y,z)$  can be used later for computing various flow parameters at any point in the flow field if there is any need for analyzing them. For that purpose an extension of WIND-02 will be needed. *This extension is not presently included but can be easily developed by the user according to his needs.*

The most important output parameters, as mentioned earlier, will appear in a printed form. The first part of the printed output of WIND-02 will give the name of the programmer, the name of the institution where the program was developed, and the name of the program. This will be followed by the listing of input data to WIND-02.

Results of the two-dimensional cascade calculations performed by subroutine GUESS will appear next. They will include the following parameters:

K          number of spanwise position of two-dimensional cylindrical surface  $(r\theta,x)$ (fig. 8)

R/RTIP    radial distance of  $K^{th}$  cylindrical surface normalized with respect to rotor radius  $r_t$

ALREL    angle between axial and rotational component of relative free-stream vector at upstream infinity, deg

TWIST    angle between chord line at  $K^{th}$  station and axis of rotation, deg

ALPHA    angle of attack at  $K^{th}$  station, deg, that is,

$$ALPHA = TWIST - ALREL$$

CL-2D    local coefficient of lift at  $K^{th}$  station (obtained by solving two-dimensional, full-potential equation on  $K^{th}$  surface)

NSUP    total number of mesh points on  $K^{th}$  surface where relative flow was locally supersonic

The values of CL-2D could serve for comparison with the standard aerodynamic results for the isolated two-dimensional airfoils in incompressible flow (ref. 14, e.g.).

Two-dimensional cascade results of subroutine GUESS are then used as an improved initial guess for the potential field in the actual three-dimensional iterative solution process of the full potential equation performed by the routine XSWEEP. For the purpose of monitoring this process the output listing from WIND-02 continues by listing the following parameters:

ITER            number of iteration sweep  
 K                number of spanwise station, that is, the number of the particular cylindrical surface intersecting the blade  
 IR, JR         (X, Y) coordinates of point where residue had largest absolute value on  $K^{th}$  surface during last iteration sweep  
 MAX.RESIDUE   maximum residue on entire two-dimensional  $K^{th}$  cylindrical surface. Its location is at the point (IR, JR, K).  
 IC, JC         (X, Y) coordinates of a point where correction to potential had maximum absolute value on  $K^{th}$  cylindrical surface during last iteration sweep  
 MAX.CORRECT   maximum value of calculated correction to potential. This correction was introduced at the point (IC, JC).  
 CIRCULATION   value of circulation  $\Gamma$  at  $K^{th}$  station  
 RELAX.COEF    value of relaxation factor RLX used in last iteration sweep at subsonic points  
 ISTG            number of leading-edge stagnation point. From that point the next iteration sweep will start proceeding along the airfoil suction surface to the trailing edge and then again from ISTG along the pressure surface to the trailing edge. In such a way the problems of marching upstream in the locally supersonic flow and the consequent introduction of negative artificial viscosity are avoided.  
 NSUP            total number of supersonic points on  $K^{th}$  surface

When the absolute value of the normalized convergence rate

$$(\Gamma^{n+1} - \Gamma^n) / \Gamma^n$$

becomes smaller than CONVER, the iterative process on that particular grid will terminate. For  $\Gamma = 0$

(when the flow is nonlifting) the iterative process on each grid will terminate after ITER = ITRMAX on that particular grid.

The printout will then be continued by listing the following values on the blade surface:

I                number (index) of point on blade surface at  $K^{th}$  station. The points are numbered clockwise starting from the trailing edge.  
 X                x coordinate of point on airfoil surface at  $K^{th}$  station  
 Y                y coordinate of point on airfoil surface at  $K^{th}$  station  
 XNORM          $x'$  coordinate normalized with local chord at  $K^{th}$  station  
 MACH           local value of relative Mach number calculated from

$$MACH = q_r / a$$

where  $q_r$  is local value of relative speed and  $a$  is local speed of sound

Q/QINF         ratio of local value of relative speed and value of relative speed measured at rotor tip radius

$$Q/QINF = q_r / (UINF^2 + OMEGA^2 * RTIP^2)^{1/2}$$

U0, V0, W0    components of local relative velocity vector along x, y and z directions, respectively

DENS            local fluid density normalized with density at upstream infinity

CPMACH also integrates the  $C_p$  distribution along the local blade sections and lists the results at each  $K^{th}$  station. The results are

FTANG          local value of aerodynamic force in  $\theta$  direction, lb

FAXIAL         local value of aerodynamic force in x direction, lb

CL-3D          three-dimensional results for sectional lift coefficient

RADIUS         radius of  $K^{th}$  station, ft

K                number (or index) of  $K^{th}$  station

CPMACH also integrates FTANG and FAXIAL in the spanwise direction and lists the total aerodynamic torque on the shaft and the total axial force on the shaft.

## Results

WIND was tested against the numerical results obtained by NASA Lewis for their ERDA-NASA

100-kilowatt Mod-0 wind turbine (refs. 15 and 16). These results were obtained for  $\Omega = 40$  rpm and  $UNIF = 18$  mph by using a code called MOSTAB (refs. 17 and 18). The blade geometry is explained in reference 15. For these same flow conditions and blade geometry WIND was tested on a single grid having  $XCELL = 24$ ,  $YCELL = 6$ ,  $ZCELL = 8$ , and  $TIPCEL = 6$  cells. Three-dimensional results obtained after only 50 iterations are presented in figure 9. It is obvious that serious errors could be made if the designer decided to use lift coefficients obtained for an isolated airfoil in free air. Even the two-dimensional cascade results (obtained by subroutine GUESS) are not acceptable for the design of wind turbine rotor blades. Two- and three-dimensional results agree very well only in the blade midspan region where the flow is essentially two dimensional. This part of the flow field is uninhibited by the three-dimensional and

compressibility effects present in the blade tip region and by the rotating cascade effects and the presence of the hub dominating the flow in the blade root region. To avoid problems and the uncertainty of dealing with the blade root effects, most designers retreat to an unimaginative method called root-cutout. It would be more beneficial to avoid such techniques in favor of using more advanced airfoils with a high critical angle of attack. In this way the aerodynamic efficiency of the rotor could be increased even for low-speed wind turbine rotors. At the same time vibration and fatigue problems caused by the flow separation in the root region could be eliminated. The three-dimensionality of the flow in the blade tip region is not inevitable if one adds properly designed winglets to the blade tip.

It is pointed out that (at least for this particular test case) the total torque on the shaft calculated by WIND was  $M_x = 24\ 680$  foot-pounds. This result agrees very well with the results for steady loading reported in references 15 and 16. The experimentally measured value of the torque was reported (ref. 16, table I(b)) to be  $M_x = 21\ 000$  foot-pounds.

An inexplicable decision by the designers of Mod-0 to place the rotor in the tower wake and consequent serious separation-induced vibrations might be a partial cause of the discrepancy between the results of WIND and the measured results in this test case.

## Concluding Remarks

A user-oriented computer program called WIND has been developed for the numerical analysis of the three-dimensional flow field about the propeller type of wind turbine rotor. WIND is an accurate and efficient computer program that is suitable for application on all nonvectorized computers. Besides final three-dimensional results, WIND also provides the results of the two-dimensional calculation so that the user can easily locate the areas of possible improvement in aerodynamic design of the blade shape. WIND is capable of reliably predicting flows that range from locally incompressible to locally supersonic, including the presence of weak shock waves.

Lewis Research Center,  
National Aeronautics and Space Administration,  
Cleveland, Ohio, May 30, 1980,  
505-32.

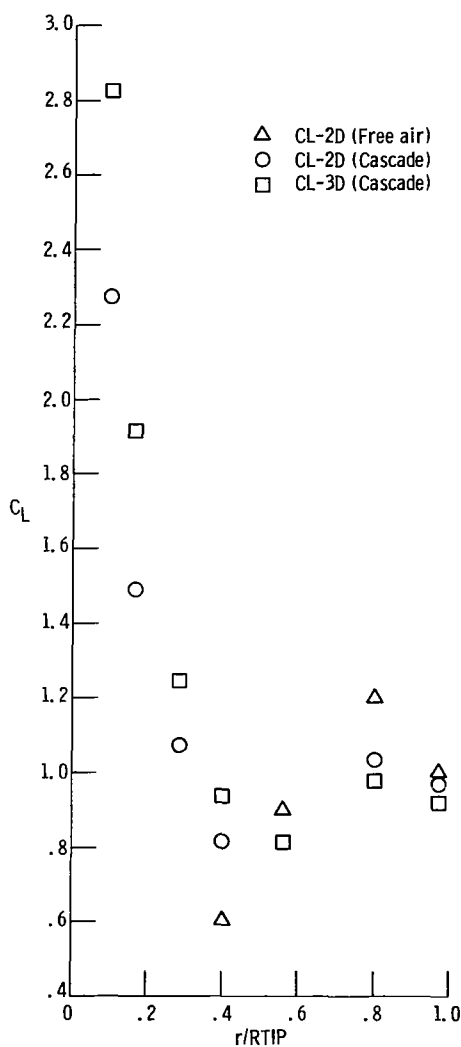


Figure 9. - Sectional values of lift distribution.

# Appendix A

## Input Data for Mod-0 Wind Turbine

```

0000100 NASA 100KW MOD-0 WIND TURBINE ; AIRFOIL NACA 2300 SERIES
0000200 XCELL = 24.000YCELL = 6.000ZCELL = 8.000TIPCEL= 6.000PMESH = 1.000
0000300 RINF = 1.200RHUB = 0.100RTIP = 62.500BLADE = 2.000SETANG= 0.000
0000400 1 0.050000 0.072000 0.006139 0.180000 0.025000 0.0000 58.0000
0000500 1 1.00000D+00 .00000D+00 111 2 .95036D+00-0.03008D+00 111
0000600 3 .90064D+00-0.05346D+00 111 4 .80116D+00-0.09606D+00 111
0000700 5 .70162D+00-0.13328D+00 111 6 .60202D+00-0.16484D+00 111
0000800 7 .50235D+00-0.18964D+00 111 8 .40256D+00-0.20556D+00 111
0000900 9 .30265D+00-0.20908D+00 111 10 .25262D+00-0.20446D+00 111
0001000 11 .20253D+00-0.19406D+00 111 12 .15001D+00-0.17704D+00 111
0001100 13 .09423D+00-0.15294D+00 111 14 .06601D+00-0.13720D+00 111
0001200 15 .03853D+00-0.11724D+00 111 16 .01331D+00-0.08864D+00 111
0001300 17 .00277D+00-0.06606D+00 111 18 .00000D+00-0.00000D+00 111
0001400 19 .00277D+00 0.08034D+00 111 20 .01331D+00 0.11528D+00 111
0001500 21 .03853D+00 0.16344D+00 111 22 .06601D+00 0.19688D+00 111
0001600 23 .09423D+00 0.22098D+00 111 24 .15001D+00 0.25056D+00 111
0001700 25 .20253D+00 0.26474D+00 111 26 .25262D+00 0.27070D+00 111
0001800 27 .30265D+00 0.27092D+00 111 28 .40256D+00 0.25856D+00 111
0001900 29 .50235D+00 0.23380D+00 111 30 .60202D+00 0.20016D+00 111
0002000 31 .70162D+00 0.15976D+00 111 32 .80116D+00 0.11374D+00 111
0002100 33 .90064D+00 0.06230D+00 111 34 .95036D+00 0.03448D+00 111
0002200 35 1.00000D+00 0.00000D+00 111 35 1.00000D+00 0.00000D+00 000
0002300 2 0.160000 0.072000 0.019645 0.120000 0.015000 0.0000 69.0000
0002400 1 1.00000D+00 .00000D+00 111 2 .95000D+00-0.02180D+00 111
0002500 3 .90000D+00-0.03880D+00 111 4 .80000D+00-0.06960D+00 111
0002600 5 .70000D+00-0.09620D+00 111 6 .60000D+00-0.11880D+00 111
0002700 7 .50000D+00-0.13620D+00 111 8 .40000D+00-0.14740D+00 111
0002800 9 .30000D+00-0.14940D+00 111 10 .25000D+00-0.14540D+00 111
0002900 11 .20000D+00-0.13720D+00 111 12 .15000D+00-0.12360D+00 111
0003000 13 .10000D+00-0.10440D+00 111 14 .07500D+00-0.09200D+00 111
0003100 15 .05000D+00-0.07600D+00 111 16 .02500D+00-0.05420D+00 111
0003200 17 .01250D+00-0.03660D+00 111 18 .00000D+00-0.00000D+00 111
0003300 19 .01250D+00 0.08180D+00 111 20 .02500D+00 0.10580D+00 111
0003400 21 .05000D+00 0.13840D+00 111 22 .07500D+00 0.16020D+00 111
0003500 23 .10000D+00 0.17660D+00 111 24 .15000D+00 0.19720D+00 111
0003600 25 .20000D+00 0.20720D+00 111 26 .25000D+00 0.21120D+00 111
0003700 27 .30000D+00 0.21100D+00 111 28 .40000D+00 0.20080D+00 111
0003800 29 .50000D+00 0.18100D+00 111 30 .60000D+00 0.15500D+00 111
0003900 31 .70000D+00 0.12360D+00 111 32 .80000D+00 0.08800D+00 111
0004000 33 .90000D+00 0.04780D+00 111 34 .95000D+00 0.02640D+00 111
0004100 35 1.00000D+00 0.00000D+00 111 35 1.00000D+00 0.00000D+00 000
0004200 3 0.240000 0.072000 0.029468 0.090000 0.009000 0.0000 75.5000
0004300 1 1.00000D+00 .00000D+00 111 2 .95000D+00-0.01800D+00 111
0004400 3 .90000D+00-0.03180D+00 111 4 .80000D+00-0.05660D+00 111
0004500 5 .70000D+00-0.07820D+00 111 6 .60000D+00-0.09620D+00 111
0004600 7 .50000D+00-0.11000D+00 111 8 .40000D+00-0.11840D+00 111
0004700 9 .30000D+00-0.11920D+00 111 10 .25000D+00-0.11560D+00 111
0004800 11 .20000D+00-0.10820D+00 111 12 .15000D+00-0.09680D+00 111
0004900 13 .10000D+00-0.08180D+00 111 14 .07500D+00-0.07220D+00 111
0005000 15 .05000D+00-0.06080D+00 111 16 .02500D+00-0.04500D+00 111
0005100 17 .01250D+00-0.03080D+00 111 18 .00000D+00-0.00000D+00 111
0005200 19 .01250D+00 0.06680D+00 111 20 .02500D+00 0.08880D+00 111
0005300 21 .05000D+00 0.11780D+00 111 22 .07500D+00 0.13800D+00 111
0005400 23 .10000D+00 0.15280D+00 111 24 .15000D+00 0.17040D+00 111
0005500 25 .20000D+00 0.17840D+00 111 26 .25000D+00 0.18160D+00 111
0005600 27 .30000D+00 0.18100D+00 111 28 .40000D+00 0.17180D+00 111
0005700 29 .50000D+00 0.15480D+00 111 30 .60000D+00 0.13220D+00 111
0005800 31 .70000D+00 0.10500D+00 111 32 .80000D+00 0.07460D+00 111
0005900 33 .90000D+00 0.04080D+00 111 34 .95000D+00 0.02240D+00 111
0006000 35 1.00000D+00 0.00000D+00 111 35 1.00000D+00 0.00000D+00 000
0006100 4 0.350000 0.065333 0.042974 0.063300 0.005000 0.0000 81.0000
0006200 1 1.00000D+00 .00000D+00 111 2 .95036D+00-0.01504D+00 111
0006300 3 .90064D+00-0.02673D+00 111 4 .80116D+00-0.04803D+00 111
0006400 5 .70162D+00-0.06664D+00 111 6 .60202D+00-0.08242D+00 111

```

0006500	7	.50235D+00-0.09482D+00	111	8	.40256D+00-0.10278D+00	111		
0006600	9	.30265D+00-0.10454D+00	111	10	.25262D+00-0.10223D+00	111		
0006700	11	.20253D+00-0.09703D+00	111	12	.15001D+00-0.08852D+00	111		
0006800	13	.09423D+00-0.07647D+00	111	14	.06601D+00-0.06860D+00	111		
0006900	15	.03853D+00-0.05862D+00	111	16	.01331D+00-0.04432D+00	111		
0007000	17	.00277D+00-0.03303D+00	111	18	.00000D+00-0.00000D+00	111		
0007100	19	.00277D+00 0.04017D+00	111	20	.01331D+00 0.05764D+00	111		
0007200	21	.03853D+00 0.08172D+00	111	22	.06601D+00 0.09844D+00	111		
0007300	23	.09423D+00 0.11049D+00	111	24	.15001D+00 0.12528D+00	111		
0007400	25	.20253D+00 0.13237D+00	111	26	.25262D+00 0.13535D+00	111		
0007500	27	.30265D+00 0.13546D+00	111	28	.40256D+00 0.12928D+00	111		
0007600	29	.50235D+00 0.11690D+00	111	30	.60202D+00 0.10008D+00	111		
0007700	31	.70162D+00 0.07988D+00	111	32	.80116D+00 0.05687D+00	111		
0007800	33	.90064D+00 0.03115D+00	111	34	.95036D+00 0.01724D+00	111		
0007900	35	1.00000D+00 0.00000D+00	111	35	1.00000D+00 0.00000D+00	000		
0008000	5	0.670000 0.038666	0.082265	0.035600	0.002500	0.0000	89.0000	
0008100	1	1.00000D+00 .00000D+00	111	2	.95000D+00-0.01090D+00	111		
0008200	3	.90000D+00-0.01940D+00	111	4	.80000D+00-0.03480D+00	111		
0008300	5	.70000D+00-0.04820D+00	111	6	.60000D+00-0.05940D+00	111		
0008400	7	.50000D+00-0.06810D+00	111	8	.40000D+00-0.07370D+00	111		
0008500	9	.30000D+00-0.07470D+00	111	10	.25000D+00-0.07270D+00	111		
0008600	11	.20000D+00-0.06860D+00	111	12	.15000D+00-0.06180D+00	111		
0008700	13	.10000D+00-0.05220D+00	111	14	.07500D+00-0.04600D+00	111		
0008800	15	.05000D+00-0.03800D+00	111	16	.02500D+00-0.02710D+00	111		
0008900	17	.01250D+00-0.01830D+00	111	18	.00000D+00-0.00000D+00	111		
0009000	19	.01250D+00 0.04090D+00	111	20	.02500D+00 0.05290D+00	111		
0009100	21	.05000D+00 0.06920D+00	111	22	.07500D+00 0.08010D+00	111		
0009200	23	.10000D+00 0.08830D+00	111	24	.15000D+00 0.09860D+00	111		
0009300	25	.20000D+00 0.10360D+00	111	26	.25000D+00 0.10560D+00	111		
0009400	27	.30000D+00 0.10550D+00	111	28	.40000D+00 0.10040D+00	111		
0009500	29	.50000D+00 0.09050D+00	111	30	.60000D+00 0.07750D+00	111		
0009600	31	.70000D+00 0.06180D+00	111	32	.80000D+00 0.04400D+00	111		
0009700	33	.90000D+00 0.02390D+00	111	34	.95000D+00 0.01320D+00	111		
0009800	35	1.00000D+00 0.00000D+00	111	35	1.00000D+00 0.00000D+00	000		
0009900	6	1.000000 0.024000	0.122784	0.015800	0.001000	0.0000	92.0000	
0010000	1	1.00000D+00 .00000D+00	111	2	.95000D+00-0.00700D+00	111		
0010100	3	.90000D+00-0.01230D+00	111	4	.80000D+00-0.02160D+00	111		
0010200	5	.70000D+00-0.03000D+00	111	6	.60000D+00-0.03670D+00	111		
0010300	7	.50000D+00-0.04170D+00	111	8	.40000D+00-0.04480D+00	111		
0010400	9	.30000D+00-0.04460D+00	111	10	.25000D+00-0.04280D+00	111		
0010500	11	.20000D+00-0.03970D+00	111	12	.15000D+00-0.03500D+00	111		
0010600	13	.10000D+00-0.02920D+00	111	14	.07500D+00-0.02610D+00	111		
0010700	15	.05000D+00-0.02260D+00	111	16	.02500D+00-0.01710D+00	111		
0010800	17	.01250D+00-0.01230D+00	111	18	.00000D+00-0.00000D+00	111		
0010900	19	.01250D+00 0.02670D+00	111	20	.02500D+00 0.03610D+00	111		
0011000	21	.05000D+00 0.04910D+00	111	22	.07500D+00 0.05800D+00	111		
0011100	23	.10000D+00 0.06430D+00	111	24	.15000D+00 0.07190D+00	111		
0011200	25	.20000D+00 0.07500D+00	111	26	.25000D+00 0.07600D+00	111		
0011300	27	.30000D+00 0.07550D+00	111	28	.40000D+00 0.07140D+00	111		
0011400	29	.50000D+00 0.06410D+00	111	30	.60000D+00 0.05470D+00	111		
0011500	31	.70000D+00 0.04360D+00	111	32	.80000D+00 0.03080D+00	111		
0011600	33	.90000D+00 0.01680D+00	111	34	.95000D+00 0.00920D+00	111		
0011700	35	1.00000D+00 0.00000D+00	111	35	1.00000D+00 0.00000D+00	000		
0011800	0	0.000000 0.000000	0.000000	0.000000	0.000000	0.0000	0.0000	

**Appendix B**  
**Input Data Format for Program WIND-01**

Card	Format
1	20A4
2 and 3	2X, 5(7X, F8.3)
4	I5, 5X, 5F10.6, 2F10.4
5 to m	I3, 2D12.5, I5, I3, 2D12.5, I5
(m + 1)	Same as card 4
.	Same as card 4 if NEXT = 222 on card m; otherwise, format is the same as on cards 5 to m
.	
n	Same as card 4

## Appendix C

### Output Listing of Program WIND-01 for Mod-0 Case

NASA 100KW MOD-0 WIND TURBINE ; AIRFOIL NACA 2300 SERIES

XCELL	YCELL	ZCELL	TIPCEL	PMESH
24.00000	6.00000	8.00000	6.00000	1.00000
RHUB	RTIP	RINF	BLADE	SETANG
0.10000	62.50000	1.20000	2.00000	0.00000

LOCAL GEOMETRIC INPUT PARAMETERS

N	RLEAD	CHORD	XLEAD	R01	R02	TLEAD	TWIST
1	0.050000	0.072000	0.006139	0.180000	0.025000	0.0000	58.0000
2	0.160000	0.072000	0.019645	0.120000	0.015000	0.0000	69.0000
3	0.240000	0.072000	0.029468	0.090000	0.009000	0.0000	75.5000
4	0.350000	0.065333	0.042974	0.063300	0.005000	0.0000	81.0000
5	0.670000	0.038666	0.082265	0.035600	0.002500	0.0000	89.0000
6	1.000000	0.024000	0.122784	0.015800	0.001000	0.0000	92.0000

CYLINDRICAL SURFACES

K	RADI1	TWIST	CHORD	XL	TL
2	0.100000E 00	0.645720E 02	0.749081E-01	0.122780E-01	0.0000
3	0.166709E 00	0.701317E 02	0.731283E-01	0.204688E-01	0.0000
4	0.286018E 00	0.786656E 02	0.709638E-01	0.351183E-01	0.0000
5	0.396563E 00	0.811770E 02	0.620590E-01	0.466227E-01	-0.0371
6	0.560923E 00	0.873103E 02	0.474956E-01	0.688719E-01	0.0000
7	0.803537E 00	0.911525E 02	0.306003E-01	0.986613E-01	0.0000
8	0.969867E 00	0.922053E 02	0.246055E-01	0.119084E 00	0.0000

DATA STORED ON UNIT NO. 10

X-Y-Z COORDINATES STORED ON UNIT 11



Appendix D  
Input Data Program WIND-02 for Mod-0 Case

```
0000100  NASA 100KW WIND TURBINE - NACA 2300 SERIES BLADE
0000200  UINF = 0.18000D+02OMEGA = 0.40000D+02TEMP = 0.32000D+02
0000300  CONVER= 1.00000D-05RLX = 1.65000D+00PMESH = 1.00000D+00
0000400  TITR1 = 0.50000D+02TITR2 = 0.10000D+02PRESS = 0.14700D+02
```

**Appendix E**  
**Input Data Format for Program WIND-02**

Card	Format
1	20A4
2, 3, and 4	2X, 3(7X, D12.5)

## References

1. Caradonna, Francis X.; and Isom, Morris P.: Supersonic and Transonic Potential Flow over Helicopter Rotor Blades. *AIAA J.*, vol. 10, no. 12, Dec. 1972, pp. 1606-1612.
2. Dulikravich, D. S.: Numerical Calculation of Inviscid Transonic Flow Through Rotors and Fans. Ph.D. Thesis, Cornell Univ., 1979.
3. Steger, J. L.; and Baldwin, B. S.: Shock Waves and Drag in the Numerical Calculation of Isentropic Transonic Flow. *NASA TN D-6997*, 1972.
4. Jameson, A.: Iterative Solution of Transonic Flows over Airfoils and Wings, Including Flows at Mach 1. *Commun. Pure Appl. Math.*, vol. 27, May 1974, pp. 283-309.
5. Jameson A.: Transonic Flow Calculations. *Computational Fluid Dynamics, Vol. 1—Numerical Analysis of Transonic and Physiological Flows. VKI-LECTURE-SERIES-87-VOL-1*. Von Karman Institute for Fluid Dynamics (Rhode-Saint-Genese, Belgium), 1976, pp. 1.1-5.84.
6. Caughey, D. A.; and Jameson, A.: Numerical Calculation of Transonic Potential Flow About Wing-Fuselage Combinations. *AIAA Paper 77-677*, June 1977.
7. Dulikravich, D. S.; and Caughey, D. A.: Finite Volume Calculation of Transonic Potential Flow Through Rotors and Fans. *FDA-80-03*, Cornell Univ., 1980.
8. Dulikravich, D. S.: Numerical Calculation of Steady Inviscid Full Potential Compressible Flow About Wind Turbine Blades. *AIAA Paper 80-0607*, 1980. (Also *NASA TM-81438*.)
9. Bauer, F.; Garabedian, P.; and Korn, D.: A Theory of Supercritical Wing Sections, with Computer Programs and Examples, *Lecture Notes in Economics and Mathematical Systems*, vol. 66. Springer-Verlag, 1972.
10. Sobieczky, H.; Fung, K. Y.; and Seebass, A. R.: A New Method for Designing Shock-Free Transonic Configurations, *AIAA Paper 78-1114*, July 1978.
11. Yu, N. J.; and Rubbert, P. E.: Acceleration Schemes for Transonic Potential Flow Calculations, *AIAA Paper 80-0338*, Jan. 1980.
12. Kober, H.: *Dictionary of Conformal Representations*. Dover Publ., Inc., 1957, p. 131.
13. Dulikravich, Djordje S.: *CAS2D—FORTRAN Program for Nonrotating, Blade-to-Blade, Steady, Potential Transonic Cascade Flows*. *NASA TP-1705*, 1980.
14. Abbott, Ira H.; von Doenhoff, Albert E.; and Stivers, Louis, S., Jr.: *Summary of Airfoil Data*. *NACA Report 824*, 1945.
15. Linscott, B.; Glasgow, J. C.; Anderson, W. D.; and Donham, R. E.: *Experimental Data and Theoretical Analysis of an Operating 100-kW Wind Turbine*, *NASA TM-73883*, 1978.
16. Kaza, K. R. J.; Janetzke, D. C.; and Sullivan, T. L.: Evaluation of MOSTAS Computer Code for Predicting Dynamic Loads in Two-Bladed Wind Turbine, *NASA TM-79101*. (Also *AIAA Paper 79-9733*.)
17. Hoffman, John A.: *User's Manual for the Modular Stability Derivative Program—High Frequency Wind Turbine Version (MOSTAB-HFW)*, *PPI-1014-8*, Paragon Pacific, Inc., 1977.
18. Spera, David A.: *Comparison of Computer Codes for Calculating Dynamic Loads in Wind Turbines*. *NASA TM-73773*, 1977.

1. Report No. <b>NASA TP-1729</b>	2. Government Accession No.	3. Recipient's Catalog No.	
4. Title and Subtitle <b>WIND - COMPUTER PROGRAM FOR CALCULATION OF THREE-DIMENSIONAL POTENTIAL COMPRESSIBLE FLOW ABOUT WIND TURBINE ROTOR BLADES</b>		5. Report Date <b>OCTOBER 1980</b>	
		6. Performing Organization Code	
7. Author(s) <b>Djordje S. Dulikravich</b>		8. Performing Organization Report No. <b>E-474</b>	
		10. Work Unit No. <b>505-32</b>	
9. Performing Organization Name and Address <b>National Aeronautics and Space Administration Lewis Research Center Cleveland, Ohio 44135</b>		11. Contract or Grant No.	
		13. Type of Report and Period Covered <b>Technical Paper</b>	
12. Sponsoring Agency Name and Address <b>National Aeronautics and Space Administration Washington, D. C. 20546</b>		14. Sponsoring Agency Code	
		15. Supplementary Notes	
16. Abstract <p>A computer program (WIND) has been developed that numerically solves an exact, full-potential equation (FPE) for three-dimensional, steady, inviscid flow through an isolated wind turbine rotor. The program automatically generates a three-dimensional, boundary-conforming grid and iteratively solves the FPE while fully accounting for both the rotating cascade and Coriolis effects. The numerical techniques incorporated involve rotated, type-dependent finite differencing, a finite volume method, artificial viscosity in conservative form, and a successive line overrelaxation combined with the sequential grid refinement procedure to accelerate the iterative convergence rate. Consequently WIND is capable of accurately analyzing incompressible and compressible flows, including those that are locally transonic and terminated by weak shocks. WIND can also be used to analyze the flow around isolated aircraft propellers and helicopter rotors in hover as long as the total relative Mach number of the oncoming flow is subsonic.</p>			
17. Key Words (Suggested by Author(s)) <b>Aerodynamics Numerical methods Wind energy Compressible flows</b>		18. Distribution Statement <b>Unclassified - unlimited STAR Category 02</b>	
19. Security Classif. (of this report) <b>Unclassified</b>	20. Security Classif. (of this page) <b>Unclassified</b>	21. No. of Pages <b>19</b>	22. Price* <b>A02</b>

\* For sale by the National Technical Information Service, Springfield, Virginia 22161